Full phenomenological consistency of the singlet-triplet scotogenic model

Andrés Rivera*, Diego Restrepo†

Instituto de Física, Universidad de Antioquia,

Calle 70 No. 52-21, Medellín, Colombia

September 26, 2018

Abstract

The singlet-triple fermion dark matter model...

1 Introduction

The singlet-triplet scotogenic model was introduced in [1]. Is a simple model that in essence combine two known models. The former is the radiative seesaw model (the scotogenic model) [2] and latter is the triplet fermion dark matter (DM) model [3]. Both models propose a good WIMP DM candidates, they gives the correct relic density in the university via the freeze-out mechanism in agreement with the value measure by the Planck satellite [4], and they are able to reproduced the parameters of the neutrino physics choosing some adequate regions of their parameter space. The single triplet fermion scotogenic model have a rich phenomenology. It has signal for WIMP nuclear-recoils, i.e. it has direct detection signal that can be testec in future experiments like XENON1T [5], LZ [6] and Darwin [7]. Something remarkable is that in the simple model proposed, it only has features for spin-independent(SI) interaction of the DM with nucleons, it is blind for spin-dependent(SD) interaction of the DM with nucleons, because it does not have interaction since the Z gauge boson. However, this observables can be generated to one loop in some region that we will aboard in this letter. Other remarkable features of this model us that it has some lepton flavor violation (LFV) processes that restring the model itself and impose strong condition in its parameter space. In particular, it have some strong restriction in radiative decays signals as $l_\alpha \to l_\beta \gamma$ in witch the principal is the $\mu \to e\,\gamma$ process, 3-body LFV decays as $\mu \to 3e$ and $\mu - e$ conversion in nuclei [8]. Even more, recently, it was shown that this model have a good consistency to high energies. Specifically, the $\mathbb{Z}_2$ symmetry that stabilizes the DM particle and ensure the radiative seesaw of the neutrino mass is preserve, i.e., is possible to have a exact $\mathbb{Z}_2$ symmetry without an spontaneous breaking in the evolution of the renormalization group equation thanks to the presence of the scalar particles inside the model [9]. In retrospective, this model is able to reproduce the DM present in our universe, it can be explain

*afelipe.rivera@udea.edu.co

†restrepo@udea.edu.co

the neutrino masses, it have a direct and indirect detection signals that can be tested in future experiments, it has LFV observables that are restricted by currently experiments and will impose strong constraints in the future, and even more, this model has a collider signals that can be tested in some experiments like the LHC [10].

After, this short introduction, the propose of this letter is to study the full consistence of all those observables at the same time. It is in this way that the model takes sense, looking for the full consistency at to some acceptable limit, i.e. our idea is to find the correct parameter space that fulfill the relic density [4], the neutrino physics parameters [11, 12], the LFV observables [8], and elastic scatter cross-section with nucleons, i.e. direct and indirect detection experiments. After that, we will show the future prospects regarding fermionic DM in this model and we will looking for some observables to 1-loop as gamma ray lines $\chi^0\chi^0 \to \gamma\gamma$ and 1-loop correction to the elastic scatter cross-section with nucleon.

The paper is organized as follows. In section 2 we introduce the model, in section 3 we do a broad search of the parameter space that is consistent with the DM, the neutrino physics an the theoretical constraints, specifically, regarding to the perturbativity of the theory and the *co-positivity* of the scalar potential(bounded from below) [9]. In section 3.1 we analyzed the direct and indirect detection status of the model and its future prospects. In section 4 we analyze the more restricted LFV processes of the model and we establish the final viable parameter space that is consistent with the multiples constraints of the model. In section 5 we compute some new observables to 1-loop of the model that could put some future constraints for the model. Specifically, in sec. 5.1 we compute the SD cross-section of DM to 1-loop and in sec. 5.2 we compute the DM annihilation into two photon, i.e. the DM DM $\to \gamma\gamma$ process. Finally, in section 6 we summarize our results, we give the conclusions and the future perspectives of the model.

2 The model

This model extend the gauge symmetry of the standard model (SM) with a new discrete $\mathbb{Z}_2$ symmetry that stabilize the DM particle. In addition to the standard model particle content, all even under the $\mathbb{Z}_2$ symmetry, the model is extend with an scalar doublet η, an real scalar triplet Ω, an two fermions with zero hypercharge, the former a singlet N and the later a triplet Σ. Their charge assignment is shown in Table 1. We follow the notation given in [8, 9]. Explicitly, the new fields are,

$$\eta = \begin{pmatrix} \eta^+ \\ \eta^0 \end{pmatrix} = \begin{pmatrix} \eta^+ \\ \frac{1}{\sqrt{2}}\left(\eta^R + i\eta^I\right) \end{pmatrix}, \quad \Omega = \begin{pmatrix} \frac{\Omega^0}{\sqrt{2}} & \Omega^+ \\ \Omega^- & -\frac{\Omega^0}{\sqrt{2}} \end{pmatrix}, \quad N, \quad \Sigma = \begin{pmatrix} \frac{\Sigma^0}{\sqrt{2}} & \Sigma^+ \\ \Sigma^- & -\frac{\Sigma^0}{\sqrt{2}} \end{pmatrix}. \tag{1}$$

The most general and invariant Lagrangian is given by

$$\begin{aligned} \mathcal{L} =& Y_e^{\alpha\beta}\bar{L}_\alpha\,\phi\,e_\beta + Y_N^\alpha\bar{L}_\alpha\,\tilde{\eta}\,N + Y_\Sigma^\alpha\bar{L}_\alpha\,\tilde{\eta}\,\Sigma + Y_\Omega\overline{\Sigma}\,\Omega\,N \\ &+\frac{1}{2}M_\Sigma\overline{\Sigma^c}\,\Sigma + \frac{1}{2}M_N\overline{N^c}N + \text{h.c.} - V(\phi,\eta,\Omega)\,, \end{aligned} \tag{2}$$

	Scalars		Fermions	
Particle	η	Ω	N	Σ
$\mathrm{SU}(2)_L$	2	3	1	3
$\mathrm{U}(1)_Y$	1/2	0	0	0
$\mathbb{Z}_2$	-	+	-	-

Table 1: New particle content and charge under the $\mathrm{SU}(2)_L \times \mathrm{U}(1)_Y \times \mathbb{Z}_2$ group.

where L and e are the fermions of the standard model, $\alpha, \beta = 1, 2, 3$, ϕ is the scalar doublet of the standard model, $\tilde{\eta} = i\sigma_2\eta^*$ as usual, and $V(\phi, \eta, \Omega)$ is the scalar potential of this new model, which is given by

$$\begin{aligned} V(\phi,\eta,\Omega) = &- m_\phi^2\phi^\dagger\phi + m_\eta^2\eta^\dagger\eta + \frac{1}{2}\lambda_1^{\mathrm{SM}}(\phi^\dagger\phi)^2 + \frac{1}{2}\lambda_2(\eta^\dagger\eta)^2 + \lambda_3(\phi^\dagger\phi)(\eta^\dagger\eta) + \lambda_4(\phi^\dagger\eta)(\eta^\dagger\phi) \\ &+ \frac{\lambda_5}{2}\left[(\phi^\dagger\eta) + \mathrm{h.c.}\right] - \frac{m_\Omega^2}{2}\,\Omega^\dagger\Omega + \frac{1}{2}\lambda_1^\Omega(\phi^\dagger\phi)(\Omega^\dagger\Omega) + \frac{1}{4}\lambda_2^\Omega(\Omega^\dagger\Omega)^2 + \frac{1}{2}\lambda^\eta(\eta^\dagger\eta)(\Omega^\dagger\Omega) \\ &+ \mu_1\,\phi^\dagger\,\Omega\,\phi + \mu_2\,\eta^\dagger\,\Omega\,\eta\,. \end{aligned} \tag{3}$$

This scalar potential is subject to some theoretical constraints. First, we demand the perturbativity of the theory, i.e. all the λ couplings needs to be ≤ 1. Second, we demand the stability of the potential, i.e. it has to be bounden from below. In this case, it have been study that the *co-positivity* of the potential is guaranteed if [9];

$$\begin{aligned} &\lambda_1 \geq 0, \qquad \lambda_2 \geq 0, \qquad \lambda_2^\Omega \geq 0, \qquad \lambda_3 + \sqrt{\lambda_1\lambda_2} \geq 0, \\ &\lambda_3 + \lambda_4 - |\lambda_5| + \sqrt{\lambda_1\lambda_2} \geq 0, \qquad \lambda_1^\Omega + \sqrt{2\lambda_1\lambda_2^\Omega} \geq 0, \qquad \lambda^\eta + \sqrt{2\lambda_2\lambda_2^\Omega} \geq 0, \\ &\sqrt{2\lambda_1\lambda_2\lambda_2^\Omega} + \lambda_3\sqrt{2\lambda_2^\Omega} + \lambda_1^\Omega\sqrt{\lambda_2} + \lambda^\eta\sqrt{\lambda_1} + \sqrt{\left(\lambda_3 + \sqrt{\lambda_1\lambda_2}\right)\left(\lambda_1^\Omega + \sqrt{2\lambda_1\lambda_2^\Omega}\right)\left(\lambda^\eta + \sqrt{2\lambda_2\lambda_2^\Omega}\right)} \geq 0\,, \end{aligned} \tag{4}$$

where we should replace λ_3 by $(\lambda_3 + \lambda_4 - |\lambda_5|)$ in the last inequality in case that $\lambda_4 + |\lambda_5| < 0$.

The symmetry breaking in this model is such that

$$\langle\phi^0\rangle = \frac{v_\phi}{2}, \qquad \langle\Omega^0\rangle = v_\Omega, \qquad \langle\eta^0\rangle = 0\,, \tag{5}$$

where the vacuum expectation values (VEVs) are itself determinate by the tadpoles equations

$$t_\phi = \frac{\partial V}{\partial v_\phi} = -m_\phi^2\,v_\phi + \frac{1}{2}\lambda_1 v_\phi^3 + \frac{1}{2}\lambda_1^\Omega v_\phi v_\Omega^2 - \frac{1}{\sqrt{2}}v_\phi v_\Omega\,\mu_1 = 0 \tag{6}$$

$$t_\Omega = \frac{\partial V}{\partial v_\Omega} = -m_\Omega^2\,v_\Omega + \lambda_2^\Omega v_\Omega^3 + \frac{1}{2}\lambda_1^\Omega v_\phi^2 v_\Omega - \frac{1}{\sqrt{2}}v_\phi^2\,\mu_1 = 0\,. \tag{7}$$

In this frame, the standard gauge boson receive new contribution to its mass, those are

$$m_W^2 = \frac{1}{4}g^2\left(v_\phi^2 + 4v_\Omega^2\right)\,, \qquad m_Z^2 = \frac{1}{4}\left(g^2 + g'^2\right)v_\phi^2\,. \tag{8}$$

In particular, the W boson mass is strongly constrained by the value of the triplet VEV, we demand that $v_\Omega < 5$ GeV [13].

2.1 $\mathbb{Z}_2$-even and $\mathbb{Z}_2$-odd spectrum

The new scalar spectrum in this model is divided in two parts. The $\mathbb{Z}_2$-even scalars ϕ^0, Ω^0, $\Omega^\pm$, $\phi^\pm$ and the $\mathbb{Z}_2$-odd scalars η^0, $\eta^\pm$, where η^0 is a good DM candidate widely studied in the literature. In this frame, the neutral scalars ϕ^0 and Ω^0 are mixed by a 2×2 mass matrix. We assume that this matrix is diagonalized with the β angle, such that

$$\begin{pmatrix} h_1 \\ h_2 \end{pmatrix} = \begin{pmatrix} \cos\beta & \sin\beta \\ -\sin\beta & \cos\beta \end{pmatrix} \begin{pmatrix} \phi^0 \\ \Omega^0 \end{pmatrix} , \tag{9}$$

The lightest h_i $\mathbb{Z}_2$-even scalar needs to be identified with the 126 GeV scalar discovered at the LHC and the heavier one remains as a new scalar higgs boson present in this theory. In the same way, the charged scalars $\phi^\pm$ and $\Omega^\pm$ are too mixed by a 2×2 mass matrix. We assume that this matrix is diagonalized with the δ angle, such that

$$\begin{pmatrix} H_1^\pm \\ H_2^\pm \end{pmatrix} = \begin{pmatrix} \cos\delta & \sin\delta \\ -\sin\delta & \cos\delta \end{pmatrix} \begin{pmatrix} \phi^\pm \\ \Omega^\pm \end{pmatrix} , \tag{10}$$

One of the $H^\pm$ charged scalar needs to be identified with the Goldstone boson usual in the standard model which is identified with longitudinal component of the W boson. The remainder is identified as a new charged scalar present in this theory. On the other hand, the $\mathbb{Z}_2$-odd scalars η^0 and $\eta^\pm$ do not mix because $\mathbb{Z}_2$ is conserved. Their masses are given by

$$m^2_{\eta^\pm} = m^2_\eta + \frac{1}{2}\lambda_3 v^2_\phi + \frac{1}{2}\lambda^\eta v^2_\Omega + \frac{1}{\sqrt{2}} v_\Omega \, \mu_2 \tag{11}$$

$$m^2_{\eta^R} = m^2_\eta + \frac{1}{2}\left(\lambda_3 + \lambda_4 + \lambda_5\right) v^2_\phi + \frac{1}{2}\lambda^\eta v^2_\Omega - \frac{1}{\sqrt{2}} v_\Omega \, \mu_2 \tag{12}$$

$$m^2_{\eta^I} = m^2_\eta + \frac{1}{2}\left(\lambda_3 + \lambda_4 - \lambda_5\right) v^2_\phi + \frac{1}{2}\lambda^\eta v^2_\Omega - \frac{1}{\sqrt{2}} v_\Omega \, \mu_2 \, . \tag{13}$$

The new fermion spectrum of the model consist of two neutral fermions χ^0_i which the lightest one can play the roll of the DM particle and one charge femion $\chi^\pm$ which comes from the charged component of the triplet fermion field Σ [1]. In this framework, the $\mathbb{Z}_2$-odd fields Σ^0 and N mixed by the Yukawa coupling Y_Ω of the eq. 2 and a non-zero VEV v_Ω. The Majorana mass matrix in the basis (Σ^0, N) is given by

$$M_\chi = \begin{pmatrix} M_\Sigma & Y_\Omega v_\Omega \\ Y_\Omega v_\Omega & M_N \end{pmatrix} , \tag{14}$$

which is diagonalized by a 2×2 matrix $V(\alpha)$, such that,

$$\begin{pmatrix} \chi^0_1 \\ \chi^0_2 \end{pmatrix} = V(\alpha) \begin{pmatrix} \Sigma^0 \\ N \end{pmatrix} = \begin{pmatrix} \cos\alpha & \sin\alpha \\ -\sin\alpha & \cos\alpha \end{pmatrix} \begin{pmatrix} \Sigma^0 \\ N \end{pmatrix} . \tag{15}$$

[1] The mass of the $\chi^\pm$ particle at tree level is given by M_Σ, however, it is known that there is a mass gap between the Σ^0 and $\Sigma^\pm$ in the pure triplet fermion model which is approximately given by the mass of the neutral pion π^0 [10, 14].

Therefore, the tree level mass for $\chi^{\pm}$ and the χ_i^0 eigenstates are

$$\begin{aligned} m_{\chi_i^0} &= M_\Sigma \\ m_{\chi_1^0} &= \frac{1}{2}\left(M_\Sigma + M_N - \sqrt{(M_\Sigma - M_N)^2 - 4(Y_\Omega v_\Omega)^2}\right) \\ m_{\chi_2^0} &= \frac{1}{2}\left(M_\Sigma + M_N + \sqrt{(M_\Sigma - M_N)^2 - 4(Y_\Omega v_\Omega)^2}\right) \end{aligned} \tag{16}$$

and the α mixing angle fulfill the relation

$$\tan(2\alpha) = \frac{2Y_\Omega v_\Omega}{M_\Sigma - M_N}\,. \tag{17}$$

2.2 Dark matter candidates

In the singlet-triplet scotogenic model we have scalars and fermionic DM particles. The lightest state charged under the $\mathbb{Z}_2$ symmetry will be a good candidate for weakly interacting DM particle.

i) Regarding scalars candidates, the lightest component of the neutral η^0 state, i.e. η^R or η^I will be the scalar DM candidate. This model has been studied extensively in the literature [15] $\cdots$, and it is known that its phenomenology is driven principally for gauge interactions which dominated the DM production in the early universe.

ii) On the other hand, the lightest χ_i^0 eigenvalue that comes from the mixing between the triplet component Σ^0 and the fermion singlet N will be the fermion DM candidate. In this case, we have a rich phenomenology that comes itself by the mixing between the singlet and the triplet fermion [1, 8, 9]. Some important features of this DM candidate are based in its nature. When it is principally singlet, i.e. when $\chi_i^0 \approx N$, the DM phenomenology is dominated by the Yukawa interactions, principally driven by the Y_N coupling of the Lagrangian 2. It implies some direct relation with LFV observables and it is so difficult to explain the relic density with Yukawa coupling to order $\mathcal{O} \lesssim 1$ [16]. On the other hand, when the DM is mostly triplet, i.e. when $\chi_i^0 \approx \Sigma^0$, its phenomenology is driven by guage interaction. In this framework is important the coanihilation with the charged fermion $\chi^{\pm}$ and it does not have serious implications in LFV observables. Even more, it is known that in this regime the correct relic density is only reproduced when the DM mass is around ~ 2.4 GeV [3]. However, some very features of the singlet-triplet mixing, perhaps the most attractive one, is that the mixing itself give us the opportunity to have a dark fermion mass in the GeV-TeV range.

   In this paper we will focus in the fermion DM case, which is the lightest eigenvalue χ_i^0 of the eq. 15. We will called it χ^0 in the developing of this work.

2.3 Neutrino masses

In this model the neutrino masses are generated to 1-loop level. They have the nature of being Majorana masses. Concretely, the mass is generated by the four diagrams schematically shown in Figure 1. Note that η^0 implies two fields, η^R, η^I and $i = 1, 2$. The neutrino mass matrix to 1-loop

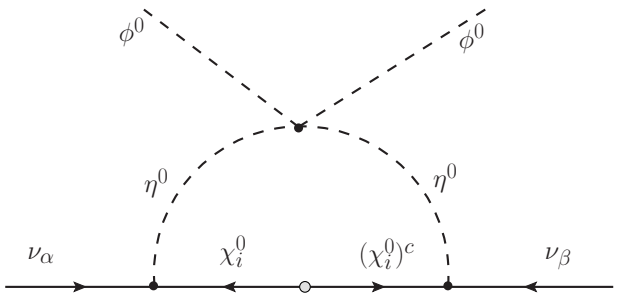

Figure 1: 1-loop diagram that generate masses in this model.

can be written as

$$(\mathcal{M}_\nu)_{\alpha\beta} = \sum_{i=1}^{2} \frac{h_{\alpha i}\, h_{\beta i}\, m_{\chi_i^0}}{2(4\pi)^2} \left[\frac{m^2_{\eta^R} \ln\left(\dfrac{m^2_{\chi_i^0}}{m^2_{\eta^R}}\right)}{m^2_{\chi_i^0} - m^2_{\eta^R}} - \frac{m^2_{\eta^I} \ln\left(\dfrac{m^2_{\chi_i^0}}{m^2_{\eta^I}}\right)}{m^2_{\chi_i^0} - m^2_{\eta^I}} \right] = \sum_{i=1}^{2} h_{\alpha i}\, \Lambda_i\, (h^T)_{i\beta} = (h\, \Lambda\, h^T)_{\alpha\beta}\,, \tag{18}$$

where h and Λ are matrices, respectively given by

$$h = \frac{1}{\sqrt{2}} \begin{pmatrix} Y^1_\Sigma & \sqrt{2}\, Y^1_N \\ Y^2_\Sigma & \sqrt{2}\, Y^2_N \\ Y^3_\Sigma & \sqrt{2}\, Y^3_N \end{pmatrix} \cdot V^T(\alpha)\,, \qquad \Lambda = \begin{pmatrix} \Lambda_1 & 0 \\ 0 & \Lambda_2 \end{pmatrix}\,, \tag{19}$$

with

$$\Lambda_i = \frac{m_{\chi_i^0}}{2(4\pi)^2} \left[\frac{m^2_{\eta^R} \ln\left(\dfrac{m^2_{\chi_i^0}}{m^2_{\eta^R}}\right)}{m^2_{\chi_i^0} - m^2_{\eta^R}} - \frac{m^2_{\eta^I} \ln\left(\dfrac{m^2_{\chi_i^0}}{m^2_{\eta^I}}\right)}{m^2_{\chi_i^0} - m^2_{\eta^I}} \right]\,. \tag{20}$$

Note that in the limit of $m_{\eta^R} = m_{\eta^I}$ we have a zero neutrino masses. This vanishing can can be understood because according with the eq. 12 and 13 it means that λ_5=0 and therefore it can be impose a conserved lepton number in this model. Even more, it can be shown that in the limit where the χ_i^0 eigenvalues are lighter that the other fields, we obtain a simple expression for the neutrino mass matrix in terms of λ_5 [1], it is

$$(\mathcal{M}_\nu)_{\alpha\beta} \approx \sum_{i=1}^{2} \frac{h_{\alpha i}\, h_{\beta i}}{(4\pi)^2} \frac{\lambda_5 v_\phi^2}{m_0^2} m_{\chi_i^0}\,, \tag{21}$$

where

$$m_0^2 = m_\eta^2 + \frac{1}{2}\,(\lambda_3 + \lambda_4)\, v_\phi^2 + \frac{1}{2}\lambda^\eta v_\Omega^2 - \frac{1}{\sqrt{2}} v_\Omega\, \mu_2 \;\Rightarrow\; m^2_{\eta^{I,R}} = m_0^2 \pm \lambda_5 v_\phi^2\,. \tag{22}$$

Parameter	Range
M_N	$1 - 10^4$ (GeV)
M_Σ	$100 - 10^4$ (GeV)
m_η	$100 - 10^4$ (GeV)
μ_i	$1 - 10^5$ (GeV)
$\lvert\lambda_i\rvert$, $\lvert\lambda_i^\Omega\rvert$, $\lvert\lambda^\eta\rvert$	$10^{-4} - 1$
v_Ω	$10^{-2} - 5$ (GeV)

Table 2: Scanning parameter ranges.

It is convenient express the Yukawas couplings $h_{\alpha i}$ in the eq. 18 using the Casas-Ibarra parametrization [17, 18]. It turns out that

$$h = U^* \sqrt{\widetilde{M}}\, R \sqrt{\Lambda}^{-1}\,, \tag{23}$$

where U is the PMNS (Pontecorvo-Maki-Nakagawa-Sakata) matrix, $\widetilde{M} = \text{diag}(m_1, m_2, m_3)$ with m_i the neutrino physical masses, Λ is given by the eq. 19 and R is a 3×2 complex, arbitrary and orthogonal matrix, such that $R\,R^T = \mathbb{I}_{3\times 3}$. The R matrix is similar to that one found in the context of type-one seesaw wit two generations of right-handed neutrinos, where we obtain one massles neutrino [18]. It depends of the neutrino hierarchy (NH: Normal hierarchy, IH: Inverse hierarchy),

$$R = \begin{pmatrix} 0 & 0 \\ \cos\gamma & \sin\gamma \\ -\sin\gamma & \cos\gamma \end{pmatrix} \quad \text{for NH}\,, \qquad R = \begin{pmatrix} \cos\gamma & \sin\gamma \\ -\sin\gamma & \cos\gamma \\ 0 & 0 \end{pmatrix} \quad \text{for IH}$$
$$m_1 \to 0 \qquad\qquad m_3 \to 0\,, \tag{24}$$

where γ is in general a complex angle.

3 The compatibility between the dark matter and neutrino physics

In order to study the DM phenomenology of this model, we scan the parameter space by considering the ranges that are shown in Table 2. We fixed m_η and $M_\Sigma > 100$ GeV in order to be conservative with LEP searches of charge particles [19] and $v_\Omega < 5$ GeV constrained by the W gauge boson mass [13]. The remaining parameters were compute from this set. In particular, m_Ω was compute using the tadpole eq. 7, λ_1^{SM} and m_ϕ^2 in the scalar potential 3 were fixed by the tadpole eq. 6 and the mass for the scalar of the standard model, $m_h \approx 125$ GeV. We did a carefully ramdom search where we imposed the theoretical constraints given by the eq. 4 and the correct Yukawa coupling Y_Σ^i, Y_N^i that reproduced the neutrino oscillation parameters [11, 12]. In order to do that, we follow the algorithm described in sec. 2.3[2]. After that, we implement this model in `SARAH` [20–24] couple to the `SPheno` [25, 26] routines. Later, we used `MicrOMEGAs 4.2.5` [27] in order to compute the relic density and we only took the models that fulfill the current value $\Omega h^2 = (0.120 \pm 0.001)$ to 3σ [4]. We

[2]We realized that neutrino hierarchy (IH, NH) does not play an important role in the analysis, for that reason we select randomly both hierarchies.

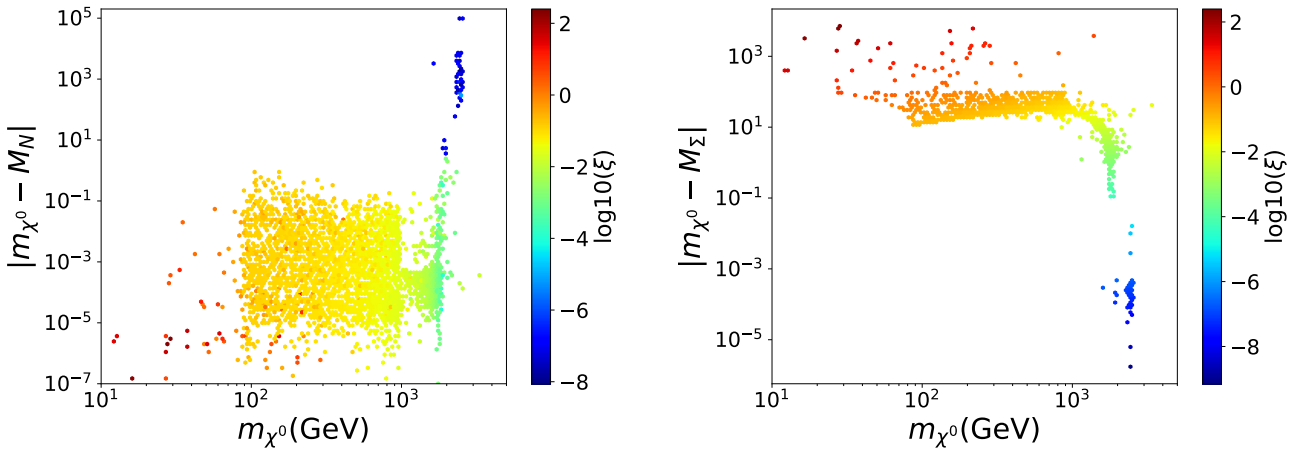

Figure 2: Parameter space that is fully consistent with DM and neutrino physics in the singlet-triplet scotogenic model. In color, we show the variable ξ define in the eq. 25. Biggers values of ξ is the limit for singlet fermion model $\sim N$ and shorts values correspond to the limit for triplet fermion DM $\sim \Sigma^0$.

realized, although the mixture between the triplet fermion Σ^0 and the singlet fermion N is important, the parameters space that is full consistent with the DM framework and the neutrino physics status, prefers a singlet component. In the left plot of Figure 2 we show that the mass of the DM particle is principally the mass of the singlet fermion M_N. Even more, in the right plot of this figure, we can see that the difference between the mass of the DM particle and the triplet fermion mass M_Σ. We realized that $|m_{\chi^0} - m_\Sigma|$ is always bigger than 10 GeV for $m_{\chi^0} < 2 \times 10^3$ GeV and for $m_{\chi^0} > 2 \times 10^3$ GeV the model recovers the known limit of the Minimal DM scenarios when the DM particle is the triplet Σ and the co-annihilation process are important. In those plots we show in color the quantity

$$\xi = \frac{|M_\Sigma - m_{\chi^0}|}{m_{\chi^0}} \tag{25}$$

that was introduce in [1] as a indicator of the behavior of the singlet-triplet mixing in all the full region.

3.1 The status of direct-indirect detection of dark matter

A tree level, this model produce direct detection signal. In particular, it has nuclear recoils, i.e. it has an spin-independent cross-section (σ_{SI}) and it is blind to spin-dependent signals because we do not have a tree level coupling between the DM and Z gauge boson. The spin-independent scattering process between the DM an the nucleon are mediated by the two higgses h_i of the model that comes from the mixing between the scalars Ω^0 and ϕ. The process is shown in Figure 3 and it is easily computed, in the limit where the Mandelstam variable t is negligible. It is given by

$$\sigma_{SI} = \frac{\mu_{\rm red}^2}{\pi} \left[\frac{M_{\rm Nuc} f_N}{v} \frac{Y_\Omega \sin(2\alpha) \sin(2\beta)}{2} \left(\frac{1}{m_{h_2}^2} - \frac{1}{m_{h_1}^2} \right) \right]^2 , \tag{26}$$

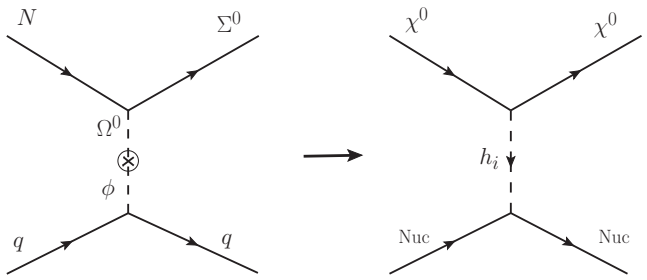

Figure 3: Spin-independent process in the singlet-triple scotogenic model. In the left, we show the process in the guage basis. In the in right, we show the process in the mass basis in order to show that actually we have to contributions coming from the two higgses h_i.

where, $M_{\rm Nuc}$ is the nucleon mass, $f_N \approx 0.3$ is the nucleon form factor, $\mu_{\rm red} = m_{\chi^0} M_{\rm Nuc}/(m_{\chi^0} + M_{\rm Nuc})$ is the reduced mass of the system and m_{h_i} is the mass of the higgs h_i.

We compute the σ_{SI} for each point of the scan that was compatible with the relic density of the DM and the neutrino physics at the same time. Even more, we did a cross-check with the `MicrOMEGAs 4.2.5` rutine [27]. Our results are shown in the left part of Figure 4 with the current experimental limits of XENON1T [5], PANDAS [28] and the LZ prospects [6]. After this, we clearly see that the scan prefers the region with a DM mass $m_{\chi^0} \gtrsim 100$ GeV. Even more, we assure that the region with low DM mass will be excluded by LFV processes as we will show in the next section. We can see that the model is no seriously restrige by the current experimental searches. Even more, the majority of the points fall into the Neutrino Coherent Scattering (NCS) [29, 30], were they will be challenging to looking for in the future. Perhaps, the most important feature is that the neutrino oscillation parameters drastically restring the parameter space of the model. After the Casas-Ibarra routine described section 2.3, the model gives us Yukawa couplings Y^i_Σ and Y^i_N all of them in the range $1^{-4} < |Y^i_{\Sigma,N}| < 1$. By construction, they reproduce the neutrino phyiscs and they reduced drastically the parameter space of the model. In order to show that, we plot in grey the contour of the naked parameter space that is only compatible with DM and was established in the ref. [1].

On the other hand, we used the `MicrOMEGAs 4.2.5` routine [27] to compute the velocity annihilation cross-section $\langle \sigma v \rangle$ of this model for each point of the scan that was compatible with the relic density of the DM and the neutrino physics at the same time. It is shown in the right part of Figure 4 with the 95% C.L gamma-ray upper limits from dSphs for DM annihilation into $b\bar{b}$ and WW [31]. As in the previous analysis, the region of low DM mas is seriously constrained by the neutrino physics. In grey, we plot the contour of the naked parameter space that is only compatible with DM and was established in the ref. [1].

4 Lepton Flavor Violation (LFV) processes

In this model we have LFV processes that seriously constrained its parameter space. Recently was shown that the most promising experiments perspectives are bases on $\mu \to 3e$, $\mu - e$ conversion in nuclei and 3-body decays $l_\beta \to l_\alpha \gamma$ which $\mu \to e\gamma$ is the most important one [8].

Before doing this analysis we take care our previous findings. In sec. 3.1 we realized that the mixing between the triplet Σ^0 and the singlet N is necessary in order to get the correct relic density

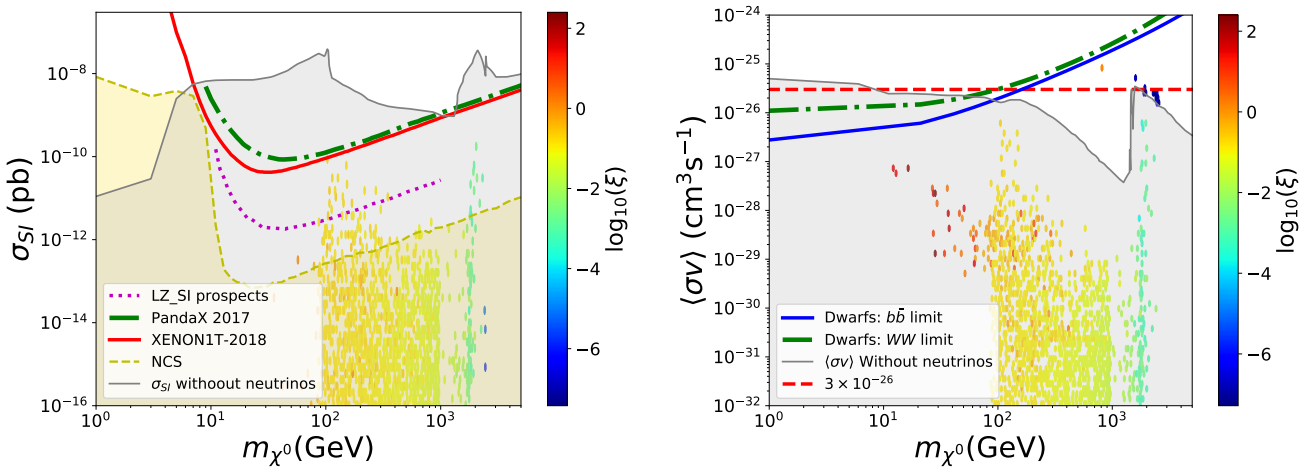

Figure 4: Left: Spin-independet cross-section. We show the currrents limits of XENON1T [5], PANDAS [28], the LZ prospects [6] and the Neutrino Coherent Scattering (NCS) [29, 30]. Right: Velocity averaged annihilation cross-section as a function of the DM mass in comparison to current indirect detection limits in different channels. The 95% C.L gamma-ray upper limits from dSphs were extracted from ref. [31]. In both plots, we show the region compatible with the relic density but without the correct Yukawas that reproduce the neutrino oscillation parameters. In colors, we plot the ξ variable defined in the eq. 25.

of the DM with a fermion mass $m_{\chi^0} < 2.7$ TeV. However, we found that in the special region with 100 GeV $< m_{\chi^0} < 1$ TeV, the eigenvalue given by the mixing is almost singlet. This was assure by the value of the ξ parameters plotted in all previous figures. Even more, we checked that mixed angle defined by the eq. 15 fulfill that $\cos\alpha \approx 0$ and $\sin\alpha \approx 1$ in this region. Therefore, we computed the $l_\beta \to l_\alpha\gamma$ process in this limit. Its principal contributions comes from the Feynman diagrams shown in Figure 5 which the left diagram with neutral fermion in the loop is common to the original scotogenic model [16, 32]. However, the diagram with the charged fermion in the loop is characteristic of this model, i.e. we have two contributions. The former comes from the mixing of the neutral fermions and the last comes from the charge fermion $\Sigma^\pm$. The branching ratio for this process is approximately

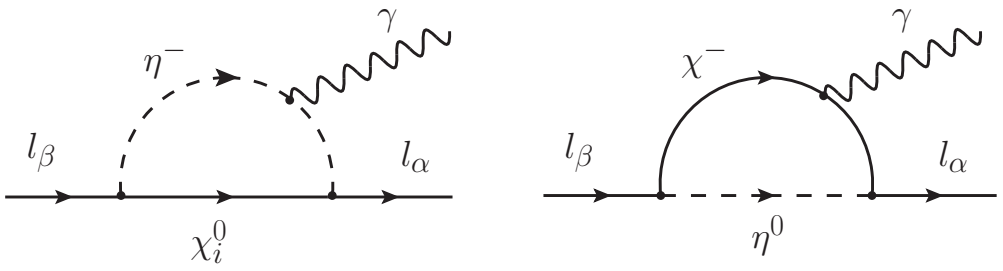

Figure 5: Dominant Feynman diagrams in the $l_\beta \to l_\alpha\gamma$ process.

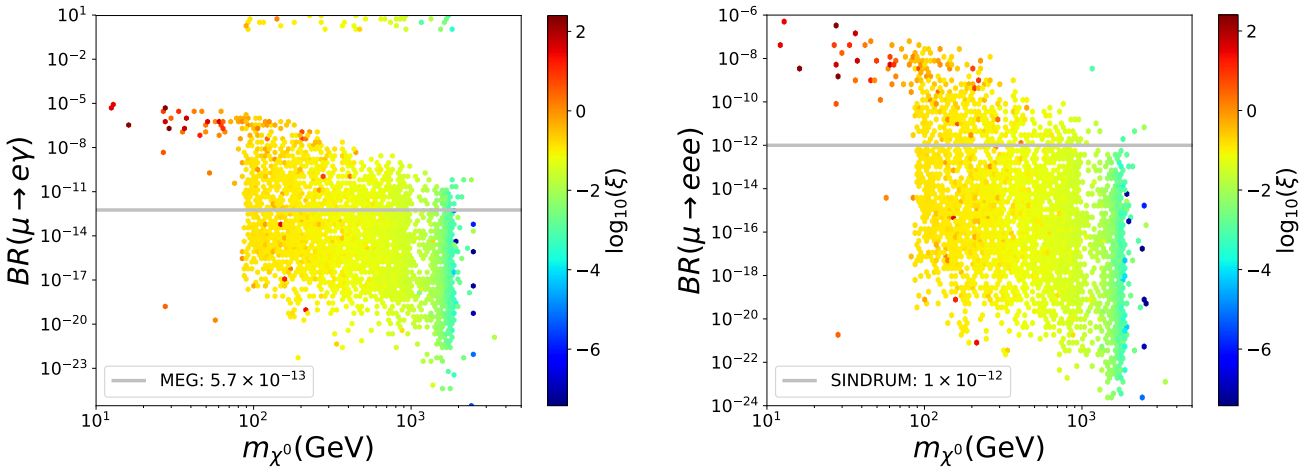

Figure 6: Left: $\mu \to e\gamma$ values for the scan of the parameter space agree with DM and the neutrino oscillation parameter. The grey line show the current limit [33], i.e. the upper region is exclude. Right: $\mu \to 3\,e$ values for the scan. The grey line show the current limit [34].

given by

$$\mathrm{Br}(l_\beta \to l_\alpha \gamma) \approx \frac{3\,\alpha_{em}\mathrm{Br}(l_\beta \to l_\alpha \nu_\beta \bar{\nu}_\alpha)}{64\,\pi G_F^2} \left| \frac{Y_{N\alpha}Y_{N\beta}^* F_2\left(\xi_1\right) + \frac{1}{2}Y_{\Sigma\alpha}Y_{\Sigma\beta}^* F_2\left(\xi_2\right)}{m_{\eta^\pm}^2} - \frac{1}{m_{\eta^0}^2}Y_{\Sigma\alpha}Y_{\Sigma\beta}^* G_2\left(\frac{m_{\chi_2^\pm}^2}{m_{\eta^0}^2}\right) \right|^2 , \tag{27}$$

where,

$$\xi_i = \frac{m_{\chi_i^0}^2}{m_{\eta^\pm}^2} \tag{28}$$

$$F_2(z) = \frac{1 - 6z + 3z^2 + 2z^3 - 6z^2 \ln z}{6(1-z)^4} \tag{29}$$

$$G_2(z) = \frac{2 + 3z - 6z^2 + z^3 + 6z \ln z}{6(1-z)^4} . \tag{30}$$

We clearly see the two contribution of the diagrams shown in Figure 5. Even more, we check that in the limit of the single scotogenic model, we recover the expression reported in the ref. [16] and in the limit of $\cos\alpha \approx 0$ we recover the expression reported in the ref. [8]. In the left part of Figure 6 we show the the behavior of the $\mu \to e\gamma$ process for the scan done in the previous section. Our analytical expression was checked with the `FalvorKit` [35] of `SARAH` [20–24] couple to the `SPheno` [25, 26] routines. Also, we show the current experimental bounds carry out by MEG experiment [33]. Even more, we compute numerically the $\mu \to 3\,e$ process which is shown in the right part of Figure 6 with its present bound given by the SINDRUM experiment [34]. We realize that some points of the parameter space are excluded, specially those with bigger ξ values. Even more, we can see that

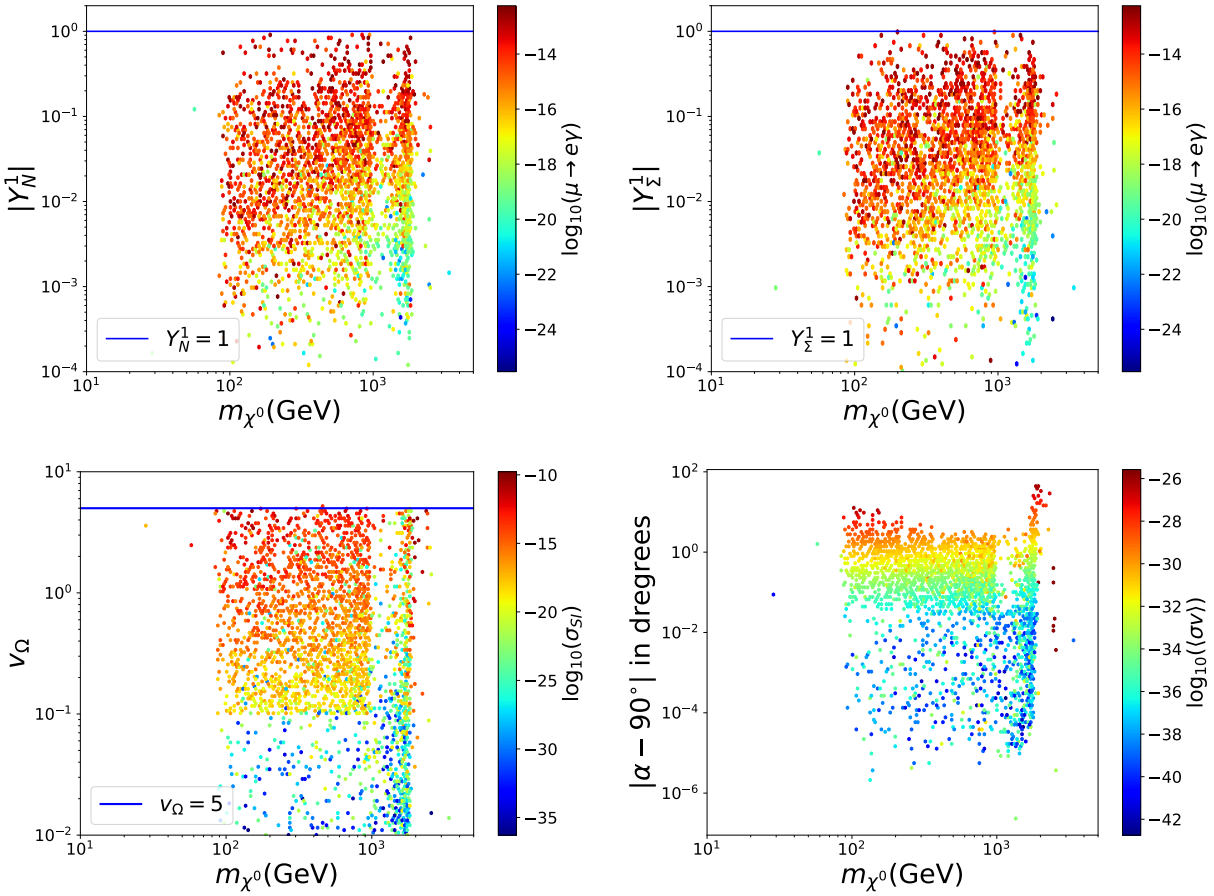

Figure 7: Behavior of the parameters of the singlet-triplet scotogenic model that fulfill DM, neutrino physics and LFV process.

although LFV processes exclude almost all the region with $m_{\chi^0} \lesssim 100$ GeV, the majority of the models with $m_{\chi^0} \gtrsim 100$ GeV survives and the previous analysis does not change significantly.

As a final part of this section, in Figure 7 we show the behavior of some of the parameters of the model that past all the last constraints According with those plots we conclude the next features. The Yukawa couplings Y_N^1 and Y_Σ^1 control the $\mu \to e\,\gamma$ process. Bigger couplings than one give us LFV in this model as we show in the up plots of the figure with similar behavior is found for all the Yukawa couplings Y_N^i and Y_Σ^i. The VEV v_Ω of the triplet scalar controls the spin-independent cross section as we expect by the construction of the model. The velocity averaged annihilation cross-section is clearly controlled by the mixing angle α defined in the ec. 15. Sizable values for $|\alpha - 90°|$ give us sizable values for the $\langle\sigma v\rangle$ as we can see in lower-right part of this figure. Even more, we assure that those are the promising points that will create bigger fluxes of gamma-ray as we will see in next section.

5 1-loop prospect processes

In this section we compute some new observables to 1-loop level in this model that are forbidden to tree level. The former is the SD cross-section of DM recoil with nuclei and the last is DM annihilation into two photons. Both of them are promising process for future signals of this model.

5.1 Spin-dependent cross-section to 1-loop

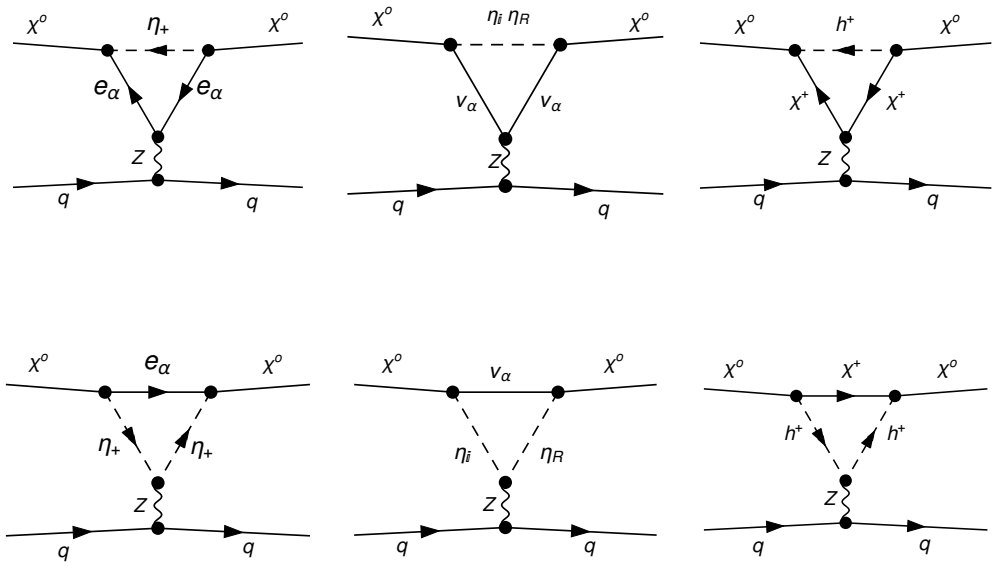

Figure 8: Diagrams contributing to SD cross-section at 1-loop level. They were generated using `FeynArts` [41].

Although this model is blind to SD scattering of DM at tree level, it can be generated at 1-loop level as is shown in Figure 8. Concretely, the exchange of the Z gauge boson leads to an effective axial vector interaction term of the form [16, 36]

$$\mathcal{L}_{\text{eff}} = \xi_q \bar{\chi^0}\gamma^\mu\gamma^5\chi^0\bar{q}\gamma_\mu\gamma^5 q + \text{h.c.}\,, \tag{31}$$

where

$$\xi_q = \frac{a_q \sin^2\alpha}{32\pi^2 M_Z^2}\left\{\sum_\alpha |Y_N^\alpha|^2\left[(v_l+a_l)\mathcal{G}_2\left(\frac{m^2_{\chi^0}}{m^2_{\eta^\pm}}\right)+(v_\nu+a_\nu)\mathcal{G}_2\left(\frac{m^2_{\chi^0}}{m_0^2}\right)\right]+Y_\Omega^2(v_\chi+a_\chi)\mathcal{G}_2\left(\frac{m^2_{\chi^0}}{m^2_{\Omega^0}}\right)\right\}, \tag{32}$$

with $a_q = \frac{1}{2}\left(-\frac{1}{2}\right)$ for $q = u,c,t\,(d,s,b)$, $a_l = -\frac{g}{2c_W}\left(\frac{1}{2}\right)$, $v_l = -\frac{g}{2c_W}\left(\frac{1}{2}-2s_W^2\right)$, $a_\nu = v_\nu =$

$\frac{g}{2c_W}\left(\frac{1}{2}\right)$, $a_\chi = 0$, $v_\chi = -g\, c_W$, $m_{h^+} \approx m_{\Omega^0}$ and $m_{\eta^R} \approx m_{\eta^I} = m_0$. $\mathcal{G}_2(z)$ is a loop function given by

$$\mathcal{G}_2(z) = -1 + \frac{2(z + (1-z)\ln(1-z))}{z^2}\,. \tag{33}$$

The resulting SD cross-section per nucleon N is given by

$$\sigma_{SD} = \frac{16}{\pi}\frac{m_{\chi^0}^2 m_N^2}{(m_{\chi^0} + m_N)^2} J_N(J_N+1)\left(\sum_{q=u,d,s}\Delta_q^N \xi_q\right)^2\,, \tag{34}$$

where $\Delta_u^N = 0.842$, $\Delta_d^N = -0.427$ and $\Delta_s^N = -0.085$ [37], m_N is the nucleon mass and J_N is the total angular momentum of the nucleus. Notice that we have three contributions to the ξ_q effective coupling. The first and the second are common to the original scotogenic model [2], however, the third one with the fermion χ^+ in the loop is characteristic of this model and could enhance the SD cross-section. Even more, we checked that in the limit of $\alpha \sim \pi/2$ and $Y_\Omega = 0$ we recovered the results found in the ref. [16]. In Figure 9 we show the behavior of the SD cross-section for all the models found in the previous section that generates the DM density via the freeze-out mechanism and saturate the value measured by the Planck satellite [4]. Also, those models generate the correct neutrino oscillation parameters [12] and are not excluded by the LFV process described in sec. 4. In this figure, we also show the IceCube [38] limits in the W^+W^- channel (black solid line) from null observations of the sun, the limits from LUX [39] (yellow solid line) and the expected sensitivity of LZ and XENON1T experiments [29](red(green) dashed(dot-dashed) line). We realize that this model is not exclude by SD scattering of DM with nuclei, however, it could be proved in the future with the next generation of experiments as LZ and XENON1T.

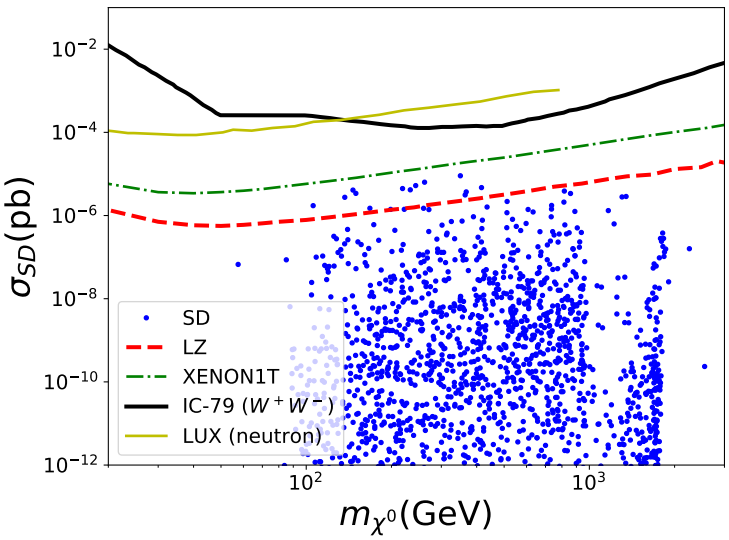

Figure 9: SD cross-section in comparison to current and future direct detection limits.

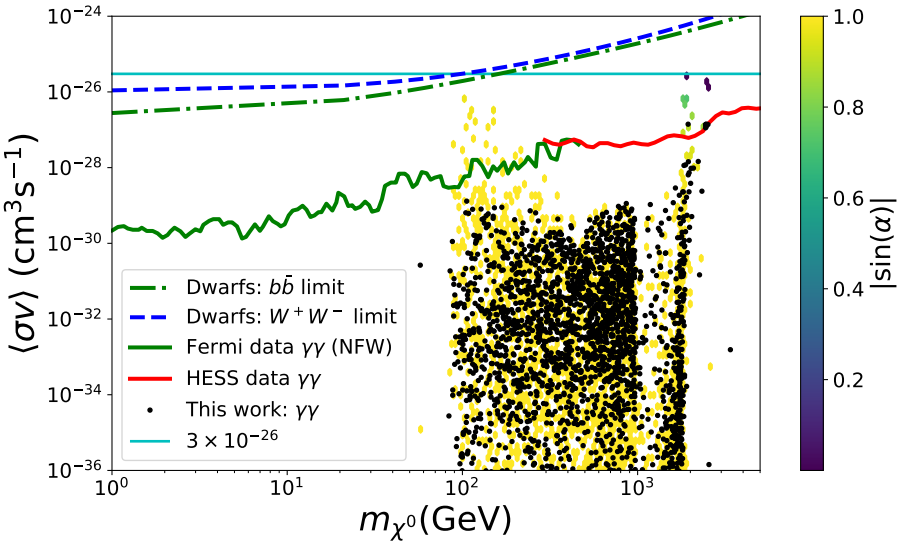

Figure 10: DM annihilation into two photon in the singlet-triplet scotogenic model.

5.2 Gamma-ray signal: DM annihilation into two photons

The DM annihilation into photons in this model is a loop process given for multiples topologies. In general, the DM annihilates into two photons ($\chi_1^0\chi_1^0 \to \gamma\gamma$) and into a photon and a one Z gauge boson ($\chi_1^0\chi_1^0 \to \gamma Z$). In this work, we compute the complete amplitude for the former process, the later one is off to the scope of this work. Following the general expression given in [40] we computed the general amplitude for the $\chi_1^0\chi_1^0 \to \gamma\gamma$ process. Even more, we use `FeynArts` [41], `FormCalc` to reduce the tensor loop integrals to scalar Passarino–Veltman functions [42] and `Package-X` [43] to compute the amplitude of this process and to do a cross-check with the general algorithm implemented in [40]. The cross-section for this process is given by

$$\sigma v(\chi_1^0\chi_1^0 \to \gamma\gamma) = \frac{|\mathcal{B}|^2}{32\pi m_{\chi_1^0}^2}\,, \tag{35}$$

where $\mathcal{B}$ is an scalar function that we will call the $\mathcal{B}$ factor. It is given in the Appendix A, eq. 36. It was written in such a way that we factorized the gauge invariant contribution in order to see the impact of the different parameters of the model. Even more, in the Appendix A we show that this general expression reproduce some known limits. For instance, in the limit of singlet fermion DM, that is, $\alpha = 90°$ and $Y_\Omega = 0$, the eq. 36 reproduced the amplitude of the scotogenic model [40, 44] as we show sec. A.1. In the same way, in the limit of pure triplet DM, that is $Y_\Omega = Y_N^\alpha = Y_\Sigma^\alpha = v_\Omega = 0$, $\alpha = 0°$ and $m = M_\Sigma$, the eq. 36 reproduce the results obtained in the high mass region for minimal DM [14] as we show in sec. A.2. After doing this check for those two known limits, we disagree with the ref. [10]. This contribution can not be extracted from a super-symmetry limit because that case does not have a pure triplet scalar Ω.

In Figure 10 we show the DM annihilation into two photons in this model. The black point in process ...

6 Conclusions

In this work we ...

7 Acknowledgments

We would like to thank ...

A General $\mathcal{B}$ factor in this model

We factorized the $\mathcal{B}$ factor in gauge invariant terms in order to get clarity in the expression

$$
\begin{aligned}
\mathcal{B} = & \frac{\sqrt{2}\alpha m^2 \sin^2(\alpha) Y_\Omega^2 (\sin(\delta)+\cos(\delta))^2}{\pi}\left[\frac{M_{H^\pm}^2 C_0\left(0,-m^2,m^2;M_{H^\pm}^2,M_{H^\pm}^2,M_\Sigma^2\right)}{M_{H^\pm}^2-M_\Sigma^2}\right. \\
& - \frac{M_\Sigma\left(-2mM_{H^\pm}^2 - M_\Sigma M_{H^\pm}^2 + m^2 M_\Sigma + 2mM_\Sigma^2 + M_\Sigma^3\right) C_0\left(0,-m^2,m^2;M_\Sigma^2,M_\Sigma^2,M_{H^\pm}^2\right)}{\left(M_{H^\pm}^2-M_\Sigma^2\right)\left(M_{H^\pm}^2+m^2-M_\Sigma^2\right)} \\
& \left. + \frac{2M_\Sigma\left(m+M_\Sigma\right) C_0\left(0,0,4m^2;M_\Sigma^2,M_\Sigma^2,M_\Sigma^2\right)}{-M_{H^\pm}^2-m^2+M_\Sigma^2}\right] \\
& + \frac{\alpha m^2 \sin(\alpha)\cos(\alpha) Y_N^\alpha Y_\Sigma^\alpha}{\pi}\left[-\frac{m_\eta^2 C_0\left(0,-m^2,m^2;m_\eta^2,m_\eta^2,m_{e_i}^2\right)}{m_\eta^2-m_{e_i}^2}\right. \\
& \left. + \frac{m_{e_i}^2\left(m_{e_i}^2+m^2-m_\eta^2\right) C_0\left(0,-m^2,m^2;m_{e_i}^2,m_{e_i}^2,m_\eta^2\right)}{\left(m_\eta^2-m_{e_i}^2\right)\left(-m_{e_i}^2+m^2+m_\eta^2\right)} + \frac{2m_{e_i}^2 C_0\left(0,0,4m^2;m_{e_i}^2,m_{e_i}^2,m_{e_i}^2\right)}{-m_{e_i}^2+m^2+m_\eta^2}\right] \\
& + \frac{\alpha m^2 \cos^2(\alpha)(Y_\Sigma^\alpha)^2}{2\sqrt{2}\pi}\left[\frac{m_\eta^2 C_0\left(0,-m^2,m^2;m_\eta^2,m_\eta^2,m_{e_i}^2\right)}{m_\eta^2-m_{e_i}^2}\right. \\
& \left. - \frac{m_{e_i}^2\left(m_{e_i}^2+m^2-m_\eta^2\right) C_0\left(0,-m^2,m^2;m_{e_i}^2,m_{e_i}^2,m_\eta^2\right)}{\left(m_\eta^2-m_{e_i}^2\right)\left(-m_{e_i}^2+m^2+m_\eta^2\right)} - \frac{2m_{e_i}^2 C_0\left(0,0,4m^2;m_{e_i}^2,m_{e_i}^2,m_{e_i}^2\right)}{-m_{e_i}^2+m^2+m_\eta^2}\right] \\
& + \frac{\sqrt{2}\alpha m^2 \sin^2(\alpha)(Y_N^\alpha)^2}{2\pi}\left[\frac{m_\eta^2 C_0\left(0,-m^2,m^2;m_\eta^2,m_\eta^2,m_{e_i}^2\right)}{m_\eta^2-m_{e_i}^2}\right. \\
& \left. - \frac{m_{e_i}^2\left(m_{e_i}^2+m^2-m_\eta^2\right) C_0\left(0,-m^2,m^2;m_{e_i}^2,m_{e_i}^2,m_\eta^2\right)}{\left(m_\eta^2-m_{e_i}^2\right)\left(-m_{e_i}^2+m^2+m_\eta^2\right)} - \frac{2m_{e_i}^2 C_0\left(0,0,4m^2;m_{e_i}^2,m_{e_i}^2,m_{e_i}^2\right)}{-m_{e_i}^2+m^2+m_\eta^2}\right] \\
& - \frac{8\sqrt{2}\alpha m^2 \cos^2(\alpha) M_W^2}{\pi\left(M_\Sigma^2-M_W^2\right)\left(4v_\Omega^2+v_\phi^2\right)\left(m^2-M_\Sigma^2+M_W^2\right)\left(m^2+M_\Sigma^2-M_W^2\right)} \\
& \left[4\left(m^2-M_W^2\right)\left(M_\Sigma^2-M_W^2\right)\left(m^2-M_\Sigma^2+M_W^2\right) C_0\left(0,0,4m^2;M_W^2,M_W^2,M_W^2\right)\right. \\
& + 2M_\Sigma\left(2m-M_\Sigma\right)\left(M_\Sigma^2-M_W^2\right)\left(m^2+M_\Sigma^2-M_W^2\right) C_0\left(0,0,4m^2;M_\Sigma^2,M_\Sigma^2,M_\Sigma^2\right) \\
& - \left(m^2-M_\Sigma^2+M_W^2\right)\left(-M_W^2\left(m^2+M_\Sigma^2\right) - 4mM_\Sigma\left(m^2+M_\Sigma^2-M_W^2\right) + 4M_\Sigma^4 + M_W^4\right) \\
& C_0\left(0,-m^2,m^2;M_W^2,M_W^2,M_\Sigma^2\right) - M_\Sigma\left(m^2+M_\Sigma^2-M_W^2\right)\left(4m^3-3m^2M_\Sigma+M_\Sigma^3-M_\Sigma M_W^2\right) \\
& \left. C_0\left(0,-m^2,m^2;M_\Sigma^2,M_\Sigma^2,M_W^2\right)\right] \qquad (36)
\end{aligned}
$$

A.1 Pure singlet dark matter (Scotogenic limit)

The $\mathcal{B}$ factor in this case can be obtained from the eq. 36 taken $\alpha = 90°$, $Y_\Omega = 0$. In this limit we have:

$$\mathcal{B} = \frac{\alpha m^2 (Y_N^\alpha)^2}{\sqrt{2}\pi}\left[\frac{m_\eta^2 C_0\left(0,-m^2,m^2;m_\eta^2,m_\eta^2,m_{e_i}^2\right)}{m_\eta^2 - m_{e_i}^2}\right.$$
$$\left. - \frac{m_{e_i}^2\left(m_{e_i}^2 + m^2 - m_\eta^2\right) C_0\left(0,-m^2,m^2;m_{e_i}^2,m_{e_i}^2,m_\eta^2\right)}{\left(m_\eta^2 - m_{e_i}^2\right)\left(-m_{e_i}^2 + m^2 + m_\eta^2\right)} - \frac{2m_{e_i}^2 C_0\left(0,0,4m^2;m_{e_i}^2,m_{e_i}^2,m_{e_i}^2\right)}{-m_{e_i}^2 + m^2 + m_\eta^2}\right] \quad (37)$$

in the limit of $m \gg m_{ei}$, i.e. when the DM mass is bigger than standard model lepton masses, this expression gives (we used `PackageX` [43])

$$\mathcal{B} = \frac{\alpha (Y_N^\alpha)^2}{2\sqrt{2}\pi}\left[\mathrm{Li}_2\left(\frac{m^2}{m_\eta^2}\right) - \mathrm{Li}_2\left(-\frac{m^2}{m_\eta^2}\right)\right]. \quad (38)$$

Therefore, using the eq. 35, we have

$$\sigma v = \frac{|\mathcal{B}|^2}{32\pi m^2} = \frac{\alpha^2 (Y_N^\alpha)^4}{256\pi^3}\left[\mathrm{Li}_2\left(\frac{m^2}{m_\eta^2}\right) - \mathrm{Li}_2\left(-\frac{m^2}{m_\eta^2}\right)\right]^2, \quad (39)$$

in agreement with [44].

A.2 Pure triplet dark matter (Minimal DM limit)

The $\mathcal{B}$ factor in this case can be obtained from the eq. 36 taken$Y_\Omega = Y_N^\alpha = Y_\Sigma^\alpha = v_\Omega = 0$, $\alpha = 0°$ and $m = M_\Sigma$. In this limit we have:

$$\mathcal{B} = \frac{8\sqrt{2}\alpha^2 m^2}{\sin(\theta_W)^2}\left[\frac{m^2\left(M_W^2 - 2m^2\right) C_0\left(0,-m^2,m^2;m^2,m^2,M_W^2\right)}{M_W^2\left(M_W^2 - m^2\right)} - \frac{2m^2 C_0\left(0,0,4m^2;m^2,m^2,m^2\right)}{M_W^2}\right.$$
$$- \frac{4\left(M_W^2 - m^2\right) C_0\left(0,0,4m^2;M_W^2,M_W^2,M_W^2\right)}{M_W^2 - 2m^2}$$
$$\left. + \frac{\left(-4m^4 + 2m^2 M_W^2 + M_W^4\right) C_0\left(0,-m^2,m^2;M_W^2,M_W^2,m^2\right)}{2m^4 - 3m^2 M_W^2 + M_W^4}\right]. \quad (40)$$

In the limit of $m \gg M_W$ we used `PackageX` [43] to get the approximated expressions for the Passarino-Veltman functions and we found that

$$\mathcal{B} \approx \frac{\sqrt{2}\pi\alpha^2 m\left(-8m^2 + \pi m M_W + 4M_W^2\right)\csc^2(\theta_W)}{M_W^3 - m^2 M_W} \quad (41)$$

and therefore, using the eq. 35, we have get that in this limit

$$\sigma v = \frac{|\mathcal{B}|^2}{32\pi m^2} \approx \frac{4\pi\alpha^4(\theta_W)}{M_W^2 \sin(\theta_W)^4}, \quad (42)$$

in agreement with [14].

References

[1] M. Hirsch, R. A. Lineros, S. Morisi, J. Palacio, N. Rojas, and J. W. F. Valle, *WIMP dark matter as radiative neutrino mass messenger*, *JHEP* **10** (2013) 149, [arXiv:1307.8134].

[2] E. Ma, *Verifiable radiative seesaw mechanism of neutrino mass and dark matter*, *Phys.Rev.* **D73** (2006) 077301, [hep-ph/0601225].

[3] E. Ma and D. Suematsu, *Fermion Triplet Dark Matter and Radiative Neutrino Mass*, *Mod. Phys. Lett.* **A24** (2009) 583–589, [arXiv:0809.0942].

[4] **Planck** Collaboration, N. Aghanim et al., *Planck 2018 results. VI. Cosmological parameters*, arXiv:1807.06209.

[5] **XENON** Collaboration, E. Aprile et al., *Dark Matter Search Results from a One Tonne× Year Exposure of XENON1T*, arXiv:1805.12562.

[6] B. J. Mount et al., *LUX-ZEPLIN (LZ) Technical Design Report*, arXiv:1703.09144.

[7] **DARWIN** Collaboration, J. Aalbers et al., *DARWIN: towards the ultimate dark matter detector*, *JCAP* **1611** (2016) 017, [arXiv:1606.07001].

[8] P. Rocha-Moran and A. Vicente, *Lepton Flavor Violation in the singlet-triplet scotogenic model*, *JHEP* **07** (2016) 078, [arXiv:1605.01915].

[9] A. Merle, M. Platscher, N. Rojas, J. W. F. Valle, and A. Vicente, *Consistency of WIMP Dark Matter as radiative neutrino mass messenger*, *JHEP* **07** (2016) 013, [arXiv:1603.05685].

[10] S. Choubey, S. Khan, M. Mitra, and S. Mondal, *Singlet-Triplet Fermionic Dark Matter and LHC Phenomenology*, *Eur. Phys. J.* **C78** (2018), no. 4 302, [arXiv:1711.08888].

[11] D. Forero, M. Tortola, and J. Valle, *Neutrino oscillations refitted*, *Phys.Rev.* **D90** (2014), no. 9 093006, [arXiv:1405.7540].

[12] P. F. de Salas, D. V. Forero, C. A. Ternes, M. Tortola, and J. W. F. Valle, *Status of neutrino oscillations 2018: 3σ hint for normal mass ordering and improved CP sensitivity*, *Phys. Lett.* **B782** (2018) 633–640, [arXiv:1708.01186].

[13] **Particle Data Group** Collaboration, K. A. Olive et al., *Review of Particle Physics*, *Chin. Phys.* **C38** (2014) 090001.

[14] M. Cirelli, N. Fornengo, and A. Strumia, *Minimal dark matter*, *Nucl. Phys.* **B753** (2006) 178–194, [hep-ph/0512090].

[15] N. G. Deshpande and E. Ma, *Pattern of Symmetry Breaking with Two Higgs Doublets*, *Phys.Rev.* **D18** (1978) 2574.

[16] A. Ibarra, C. E. Yaguna, and O. Zapata, *Direct Detection of Fermion Dark Matter in the Radiative Seesaw Model*, *Phys. Rev.* **D93** (2016), no. 3 035012, [arXiv:1601.01163].

[17] J. A. Casas and A. Ibarra, *Oscillating neutrinos and muon —¿ e, gamma*, *Nucl. Phys.* **B618** (2001) 171–204, [hep-ph/0103065].

[18] A. Ibarra and G. G. Ross, *Neutrino phenomenology: The Case of two right-handed neutrinos*, *Phys.Lett.* **B591** (2004) 285–296, [hep-ph/0312138].

[19] **SLD Electroweak Group, DELPHI, ALEPH, SLD, SLD Heavy Flavour Group, OPAL, LEP Electroweak Working Group, L3** Collaboration, S. Schael et al., *Precision electroweak measurements on the Z resonance*, *Phys. Rept.* **427** (2006) 257–454, [hep-ex/0509008].

[20] F. Staub, *SARAH*, arXiv:0806.0538.

[21] F. Staub, *From Superpotential to Model Files for FeynArts and CalcHep/CompHep*, *Comput. Phys. Commun.* **181** (2010) 1077–1086, [arXiv:0909.2863].

[22] F. Staub, *Automatic Calculation of supersymmetric Renormalization Group Equations and Self Energies*, *Comput. Phys. Commun.* **182** (2011) 808–833, [arXiv:1002.0840].

[23] F. Staub, *SARAH 3.2: Dirac Gauginos, UFO output, and more*, *Comput. Phys. Commun.* **184** (2013) 1792–1809, [arXiv:1207.0906].

[24] F. Staub, *SARAH 4: A tool for (not only SUSY) model builders*, *Comput.Phys.Commun.* **185** (2014) 1773–1790, [arXiv:1309.7223].

[25] W. Porod, *SPheno, a program for calculating supersymmetric spectra, SUSY particle decays and SUSY particle production at e+ e- colliders*, *Comput. Phys. Commun.* **153** (2003) 275–315, [hep-ph/0301101].

[26] W. Porod and F. Staub, *SPheno 3.1: Extensions including flavour, CP-phases and models beyond the MSSM*, *Comput.Phys.Commun.* **183** (2012) 2458–2469, [arXiv:1104.1573].

[27] G. Belanger, F. Boudjema, A. Pukhov, and A. Semenov, *MicrOMEGAs 2.0: A Program to calculate the relic density of dark matter in a generic model*, *Comput.Phys.Commun.* **176** (2007) 367–382, [hep-ph/0607059].

[28] **PandaX-II** Collaboration, X. Cui et al., *Dark Matter Results From 54-Ton-Day Exposure of PandaX-II Experiment*, *Phys. Rev. Lett.* **119** (2017), no. 18 181302, [arXiv:1708.06917].

[29] P. Cushman et al., *Working Group Report: WIMP Dark Matter Direct Detection*, in *Community Summer Study 2013: Snowmass on the Mississippi (CSS2013) Minneapolis, MN, USA, July 29-August 6, 2013*, 2013. arXiv:1310.8327.

[30] J. Billard, L. Strigari, and E. Figueroa-Feliciano, *Implication of neutrino backgrounds on the reach of next generation dark matter direct detection experiments*, *Phys. Rev.* **D89** (2014), no. 2 023524, [arXiv:1307.5458].

[31] **Fermi-LAT** Collaboration, M. Ackermann et al., *Searching for Dark Matter Annihilation from Milky Way Dwarf Spheroidal Galaxies with Six Years of Fermi-LAT Data*, arXiv:1503.02641.

[32] T. Toma and A. Vicente, *Lepton Flavor Violation in the Scotogenic Model*, *JHEP* **1401** (2014) 160, [arXiv:1312.2840].

[33] **MEG** Collaboration, J. Adam et al., *New constraint on the existence of the $\mu^+ \to e^+\gamma$ decay*, *Phys.Rev.Lett.* **110** (2013) 201801, [arXiv:1303.0754].

[34] **SINDRUM** Collaboration, W. H. Bertl et al., *Search for the Decay $\mu^+ \to e^+e^+e^-$*, *Nucl. Phys.* **B260** (1985) 1–31.

[35] W. Porod, F. Staub, and A. Vicente, *A Flavor Kit for BSM models*, *Eur.Phys.J.* **C74** (2014), no. 8 2992, [arXiv:1405.1434].

[36] G. Jungman, M. Kamionkowski, and K. Griest, *Supersymmetric dark matter*, *Phys. Rept.* **267** (1996) 195–373, [hep-ph/9506380].

[37] **HERMES** Collaboration, A. Airapetian et al., *Precise determination of the spin structure function g(1) of the proton, deuteron and neutron*, *Phys. Rev.* **D75** (2007) 012007, [hep-ex/0609039].

[38] M. G. Aartsen, R. Abbasi, Y. Abdou, M. Ackermann, J. Adams, J. A. Aguilar, M. Ahlers, D. Altmann, J. Auffenberg, X. Bai, and et al., *Search for Dark Matter Annihilations in the Sun with the 79-String IceCube Detector*, *Physical Review Letters* **110** (Mar., 2013) 131302, [arXiv:1212.4097].

[39] **LUX** Collaboration, D. S. Akerib et al., *First spin-dependent WIMP-nucleon cross section limits from the LUX experiment*, arXiv:1602.03489.

[40] C. Garcia-Cely and A. Rivera, *General calculation of the cross section for dark matter annihilations into two photons*, *JCAP* **1703** (2017), no. 03 054, [arXiv:1611.08029].

[41] T. Hahn, *Generating Feynman diagrams and amplitudes with FeynArts 3*, *Comput. Phys. Commun.* **140** (2001) 418–431, [hep-ph/0012260].

[42] G. Passarino and M. Veltman, *One Loop Corrections for e+ e- Annihilation Into mu+ mu- in the Weinberg Model*, *Nucl.Phys.* **B160** (1979) 151.

[43] H. H. Patel, *Package-X: A Mathematica package for the analytic calculation of one-loop integrals*, *Comput. Phys. Commun.* **197** (2015) 276–290, [arXiv:1503.01469].

[44] M. Garny, A. Ibarra, and S. Vogl, *Signatures of Majorana dark matter with t-channel mediators*, *Int. J. Mod. Phys.* **D24** (2015), no. 07 1530019, [arXiv:1503.01500].